

# UCLA

## UCLA Previously Published Works

### Title

Fluorinated Thieno[2',3':4,5]benzo[1,2-d][1,2,3]triazole: New Acceptor Unit To Construct Polymer Donors

### Permalink

<https://escholarship.org/uc/item/7mz7x9zq>

### Journal

ACS Omega, 3(10)

### ISSN

2470-1343

### Authors

Jiang, Xiu  
Wang, Jiacheng  
Yang, Yang  
et al.

### Publication Date

2018-10-31

### DOI

10.1021/acsomega.8b02053

Peer reviewed

# Fluorinated Thieno[2',3':4,5]benzo[1,2-*d*][1,2,3]triazole: New Acceptor Unit To Construct Polymer Donors

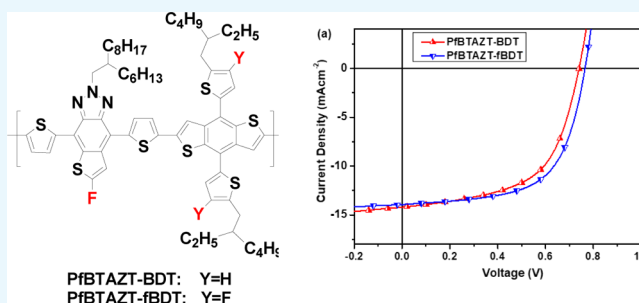
Xiu Jiang,<sup>†</sup> Jiacheng Wang,<sup>†</sup> Yang Yang,<sup>†</sup> Xiaowei Zhan,<sup>\*,‡</sup> and Xingguo Chen<sup>\*,†</sup>

<sup>†</sup>Hubei Key Laboratory on Organic and Polymeric Opto-Electronic Materials, College of Chemistry and Molecular Sciences, Wuhan University, Wuhan 430072, China

<sup>‡</sup>Department of Materials Science and Engineering, College of Engineering, Peking University, Beijing 100871, China

## Supporting Information

**ABSTRACT:** A new acceptor unit, fluorinated thieno[2',3':4,5]benzo[1,2-*d*][1,2,3]triazole (fBTAZT), has been designed and synthesized to build two donor–acceptor (D–A) copolymers with the none/fluorinated benzodithiophene (BDT) unit, which have been applied as the electron-donating material with ITIC as an electron-accepting material to fabricate the nonfullerene polymer solar cells (PSCs). It is found that fluorination at the BTAZT unit and BDT unit exerts a significant influence on photophysical properties and photovoltaic performances of the PSCs. As a result, when the fluorine atom is introduced both into the BTAZT unit and the side-chain thiophene ring of the BDT unit, the corresponding polymer P<sub>f</sub>BTAZT-fBDT exhibits deeper highest occupied molecular orbital–lowest unoccupied molecular orbital energy level and shows stronger interchain interaction with a little broad and red-shift absorption and high charge mobilities as well as good phase-separated morphologies, thus leading to higher power conversion efficiency of 6.59% in nonfullerene PSCs compared with another polymer P<sub>f</sub>BTAZT-BDT without F atom at the BDT unit, indicating that fBTAZT can be acted as a medium strong organic acceptor to build D–A polymer donor for high efficient PSCs.



## INTRODUCTION

Polymer solar cells (PSCs) as a new energy have got a lot of attention because of their great merits of being lightweight, constitute flexible, and low-cost fabrication.<sup>1–7</sup> Much recently, the power conversion efficiency (PCE) of PSCs has been boosted from over 10–11%<sup>8,9</sup> up to over 13–14%<sup>10–16</sup> in single junction solar cells with a medium or wide band gap-conjugated polymer as a donor and narrow band gap n-type organic semiconductor (n-OS) as an acceptor. At present, a series of narrow band gap n-OS acceptors with excellent performance,<sup>17–33</sup> such as ITIC,<sup>34</sup> IEIC,<sup>35</sup> and IDIC,<sup>36,37</sup> have been reported. With the rapid development of the narrow band gap n-OS acceptors, medium or wide band gap D–A polymeric donors draw the attention because of the complementary absorption for efficiently harvesting sunlight.<sup>38,39</sup> The D–A copolymers based on the bithienylbenzodithiophene-*alt*-benzotriazole (BTA) backbone have been confirmed as highly efficient donor materials for nonfullerene PSCs.<sup>40–44</sup> For D–A polymer designing,<sup>45</sup> side-chain engineering was often used to the molecular design,<sup>46</sup> especially for fluorine (F). In addition, a number of groups have verified that the introduction of F atom into BTA units or the conjugated side groups of the BDT unit is an effective strategy to raise PCE of the PSCs because of the electronegative effect of F atom and intermolecular interactions between F atom and other atoms.<sup>47–50</sup> These may produce a deep highest occupied

molecular orbital (HOMO) energy level for a high open-circuit voltage ( $V_{oc}$ ) of the PSCs and ordered crystalline structure for a high hole mobility. For example, Li et al.<sup>51</sup> had reported a wide band gap polymer donor named J91, in which the introduction of two F atoms into the BTA unit and four F atoms into the side groups of the BDT unit resulted in great enhancement of the PCE from 4.80% of the polymer J50 without F atoms to 11.63% of the polymer J91. Interestingly, it seems that the introduction of one or more F atoms onto the donor unit or/and acceptor unit of D–A copolymers may result in a distinct influence on the photovoltaic performance.<sup>52–55</sup> For example, Hou and co-workers<sup>56</sup> developed four D–A copolymers based on BDT and thieno[3,4-*b*]thiophene (TT) to investigate the influence of F atoms at different positions on the photovoltaic performances. The results indicated that when one or more F atoms were attached to the BDT unit or TT unit, the photovoltaic performances of the polymer-based PSCs were varied greatly. Therefore, how to extend the application of fluorination in D–A polymers is still interesting and is also of significant importance to the molecular design of highly efficient photovoltaic polymers.

Received: August 15, 2018

Accepted: October 9, 2018

Published: October 23, 2018

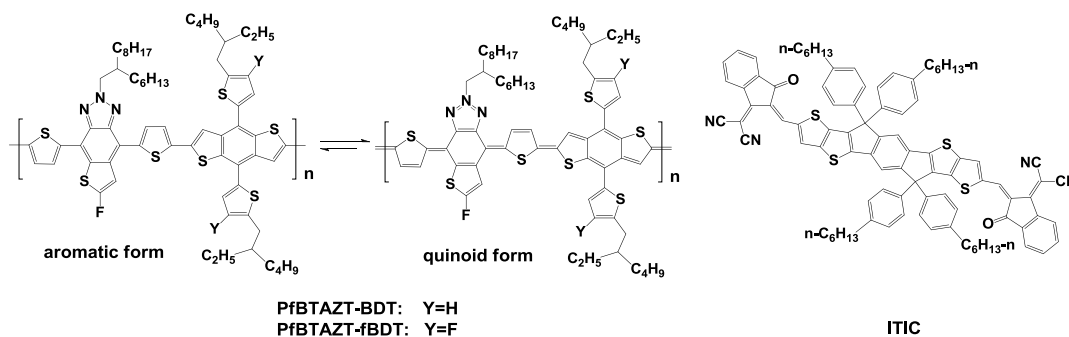
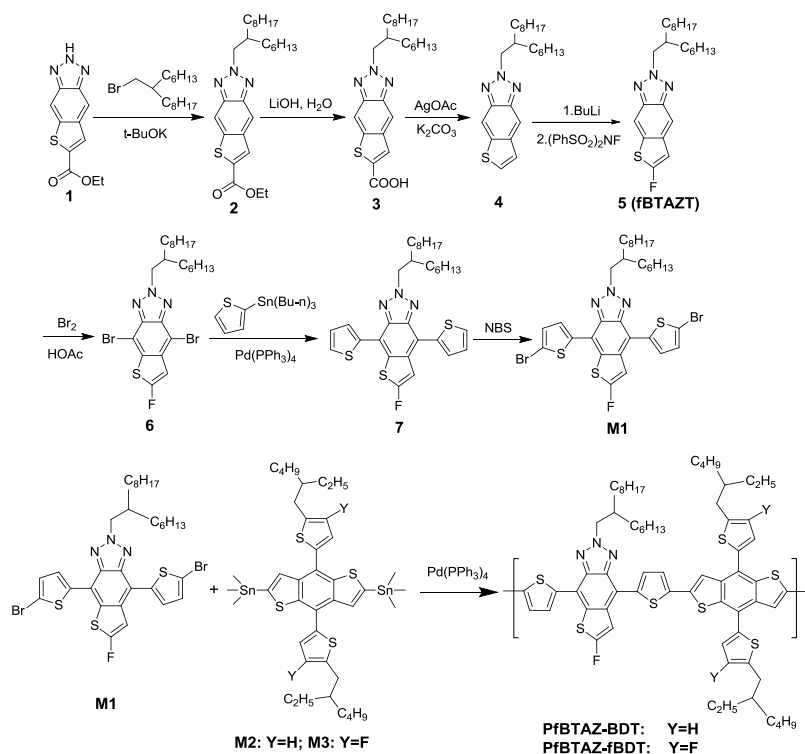


**Figure 1.** Structure of the polymers and ITIC.

**Scheme 1. Synthetic Routes for fBTAZT, Monomer (M1), and Polymers**



Recently, our group had reported several organic acceptors, such as thiophene-fused benzotriazole (BTAZT) and thiophene-fused benzothiadiazole (BTT), to build D–A copolymers for PSCs. It has been found that the fusion of one thiophene ring at the side of BTAZ or BT unit can stabilize the quinoid population of the D–A conjugation backbone, thus to strengthen the intramolecular charge-transfer (ICT) effect and promote the short-circuit current density ( $J_{sc}$ ).<sup>57–59</sup> Therefore, in this work, a new BTA-based organic acceptor, fluorinated thieno[2',3':4,5]benzo[1,2-d][1,2,3]triazole (fBTAZT), has been designed, in which fluorine (F) is introduced at  $\alpha$ -position of the fused thiophene ring at the BTAZT unit to further regulate HOMO–lowest unoccupied molecular orbital (LUMO) energy levels and the photophysical properties. Then, two D–A copolymers have been synthesized based on the fBTAZT unit with BDT and fluorinated BDT units, respectively, which are named PfbTAZT-BDT and PfbTAZT-fBDT and shown in Figure 1. Furthermore, the introduction of F atoms at BTAZT or/and BDT units to influence the photophysical and electrochemical properties of the polymers as well as the photovoltaic performances of the PSCs has been

investigated. It is found that fluorination at BTAZT and BDT units exerts a synergistic effect on the HOMO–LUMO energy levels and photovoltaic performances of the corresponding D–A copolymers. Indeed, the polymer PfbTAZT-fBDT introduced fluorine atoms at both BTAZT and BDT blocks shows the deeper HOMO level, and the corresponding solar cell device exhibits a relatively high  $V_{oc}$  of 0.77 V and PCE of 6.59%.

## RESULTS AND DISCUSSION

**Synthesis and Characterization.** In this work, fBTAZT as a new organic acceptor has been designed and Scheme 1 presents the synthetic process of fBTAZT unit and two polymers (PfbTAZT-BDT and PfbTAZT-fBDT). As shown, the initial compounds 1 and 2 (yield, 28.7%) were synthesized according to the previous paper reported by our group.<sup>55</sup> Then, the hydrolysis of 2 produced ethyl 2-(2-hexyldecyl)-2H-thieno[2',3':4,5]benzo[1,2-d][1,2,3]triazole-6-carboxylate (3) (yield, 95%), and the thermal decarboxylation of 3 yielded the important immediate compound 4 (yield, 87.3%), 2-(2-hexyldecyl)-2H-thieno[2',3':4,5]benzo[1,2-d][1,2,3]triazole

**Table 1. Optical and Physical Properties of PfbTAZT-BDT and PfbTAZT-fBDT**

polymer	$M_n$ (PDI) (kDa)	$T_d$ ( $^{\circ}\text{C}$ )	$\lambda_{\text{max}}^{\text{soln}}$ (nm)	$\lambda_{\text{max}}^{\text{film}}$ (nm)	$E_{\text{HOMO}}^b$ (eV)	$E_{\text{LUMO}}^c$ (eV)	$E_{\text{g}}^{\text{opt}d}$ (eV)
PfbTAZT-BDT	94(2.4)	420	348, 571	351, 577	-5.27	-3.45	1.82
PfbTAZT-fBDT	85(2.5)	431	350, 580	353, 579	-5.37	-3.58	1.79

<sup>a</sup>Polymer thin films on the quartz plate cast from chloroform solution. <sup>b</sup> $E_{\text{HOMO}} = -(4.80 + E_{\text{ox}}^{\text{onset}} - 0.49)$ . <sup>c</sup> $E_{\text{LUMO}} = E_{\text{HOMO}} - E_{\text{g}}^{\text{opt}}$ . <sup>d</sup>Calculated from the absorption edge of the polymer films:  $E_{\text{g}}^{\text{opt}} = 1240/\lambda^{\text{edg}}$ .

(BTAZT). Afterward, under the protection of argon, butyl lithium was applied to remove hydrogen from the  $\alpha$ -position of the fused thiophene at BTAZT and the fluorinating reagent (PhSO<sub>2</sub>)<sub>2</sub>NF was added to complete the fluorination to yield 6-fluoro-2-(2-hexyldecyl)-2H-thieno[2',3':4,5]benzo[1,2-*d*]-[1,2,3]triazole (fBTAZT) (**5**) (yield, 59.1%), which can be acted as a new organic acceptor unit to construct the D–A copolymer. The rest of the compounds and final monomer (**M1**) were synthesized according to the previous paper reported by our group. The detailed synthetic process is shown in the Supporting Information, and all of the compounds were identified by NMR and mass spectrometry. Monomers **M2** and **M3** were prepared according to the procedure described in the literature.<sup>60</sup> Finally, two copolymers (PfbTAZT-BDT and PfbTAZT-fBDT) based on fBTAZT and BDT or fBDT units were synthesized via Stille coupling reaction of **M1** with **M2** or **M3**, respectively, and the detailed synthetic process is shown in the Supporting Information. These two polymers are easily soluble in some usual organic solvents such as tetrahydrofuran, chloroform, chlorobenzene, toluene, and so on. The number-average molecular weights ( $M_n$ ) and polydispersity indices (PDIs) were measured by gel permeation chromatography analysis, and the corresponding data are listed in Table 1. The thermal stability of the two polymers was tested by the thermogravimetric analysis (TGA). Both of them showed very fine thermal stability with 5% weight loss beyond 400  $^{\circ}\text{C}$  (Table 1 and Figure S1).

**Optical Properties.** Figure 2 shows the UV–vis absorption spectra of the polymers in dilute chloroform solution and in

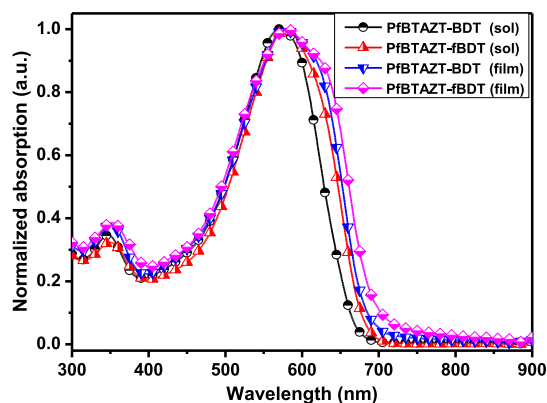


**Figure 2.** UV–vis spectra of PfbTAZT-BDT and PfbTAZT-fBDT in CHCl<sub>3</sub> solution and in thin film.

the thin film, and the corresponding data are summarized in Table 1. As can be seen, both in the solution and in thin film, PfbTAZT-BDT and PfbTAZT-fBDT display the similar absorption spectra with two broad bands in the region of 300–400 and 400–700 nm, respectively. The high-energy band of 300–400 nm is related to the local  $\pi$ – $\pi^*$  electron transition of conjugated skeleton, and the low-energy band with stronger absorption in 400–700 nm can be attributed to

the ICT effect. It should be noted that PfbTAZT-fBDT only exhibits a little red-shift absorption compared with PfbTAZT-BDT both in solution and in thin film. In addition, the absorption in the thin film also exhibits a little red shift compared with that in solution for both PfbTAZT-BDT and PfbTAZT-fBDT. This indicates that there is a strong interchain interaction between the conjugation backbones in solution and in solid state. As shown in Figure 1, PfbTAZT-BDT has a little structural difference from PfbTAZT-fBDT where another F atom has been introduced into the side-chain thiophene ring of the BDT unit. It seems that the F atom with pair electrons at the backbone of PfbTAZT-fBDT shows weak electron-donating ability to increase the  $\pi$ -electron density of BDT, thus to strengthen the ICT effect from the electron-donating unit (fBDT) to electron-accepting unit (fBTAZT). At the same time, the presence of more F atoms at the conjugation backbone is favorable to strengthen the intermolecular interaction among the polymeric main chains, which can also lead to the red-shift absorption. Moreover, the fusion of a thiophene ring into the BTAZT unit can stabilize the quinoid structure of the conjugation backbone and enhance the rigidity of the main-chain conjugation backbone,<sup>61,62</sup> which is beneficial for the interchain  $\pi$ – $\pi$  interaction, so these two polymers only exhibit a little different absorption both in solution and in solid state. Therefore, it is inferred that synergy of the fusion of the thiophene ring onto the BTAZT unit and the introduction of F atom at the BDT unit are attributed to different absorption properties between PfbTAZT-BDT and PfbTAZT-fBDT. The absorption edges of PfbTAZT-BDT and PfbTAZT-fBDT from the absorption spectra in the thin film are estimated to be about 681 and 693 nm, respectively, which corresponds to the optical band gaps ( $E_{\text{g}}^{\text{opt}}$ ) of 1.82 and 1.79 eV. This indicates that fluorination onto the conjugated side groups of the BDT unit can slightly decrease the band gap of the polymer<sup>42</sup> and both of them belong to the medium band gap semiconductors.

In addition, the extinction coefficient of PfbTAZT-BDT and PfbTAZT-fBDT in CHCl<sub>3</sub> solution has been measured, as shown in Figure S3 (Supporting Information). It can be seen that PfbTAZT-fBDT shows the weaker absorption efficiency in the region of 450–700 nm compared with PfbTAZT-BDT, although it has a little red-shift ICT absorption band.

**Electrochemical Properties.** The HOMO levels of these two polymers were studied by cyclic voltammetry (CV) measurement, as shown in Figure 3, and the electrochemical data are also summarized in Table 1.

As can be seen from Figure 3, the onset oxidation potentials of PfbTAZT-BDT and PfbTAZT-fBDT were estimated to be about 0.94 and 1.04 V, respectively. The corresponding HOMO energy levels were determined to be -5.27 eV for PfbTAZT-BDT and -5.37 eV for PfbTAZT-fBDT. At the same time, the corresponding LUMO energy levels of PfbTAZT-BDT and PfbTAZT-fBDT are also estimated to be about -3.45 and -3.58 eV, respectively, coming from the difference between the HOMO energy level and the optical

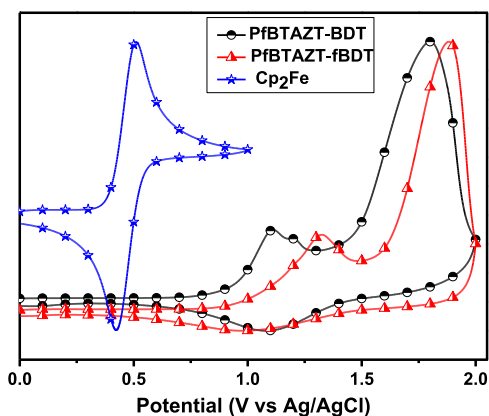


Figure 3. CV curves of PfbTAZT-BDT and PfbTAZT-fBDT.

band gap (shown in Table 1). Because of very strong electronegativity of F atom, the import of F atom onto the conjugation backbone has become one of the effective strategies to regulate the HOMO–LUMO energy level of the acceptor or donors for enhancing the open voltage ( $V_{oc}$ ), and to strengthen the intermolecular interaction for improving the charge mobility and further increasing the short-circuit current density ( $J_{sc}$ ) of the PSCs. Obviously, in this work, the introduction of two F atoms both onto the BTAZT unit and the side-chain thiophene ring of BDT unit makes PfbTAZT-fBDT which shows much lower HOMO–LUMO energy levels than PfbTAZT-BDT. Generally, the lower HOMO energy level is more beneficial to achieve higher  $V_{oc}$  in the PSCs, which has been observed in the following investigation for the polymer-based PSCs.

The photoluminescence (PL) quenching experiments have been performed to investigate the charge-transfer behavior in the polymer/ITIC blend films (Figure S4). As can be seen, when excited at 700 nm, the PL of ITIC was almost completely quenched when blended with PfbTAZT-BDT or PfbTAZT-fBDT, suggesting that there is efficient hole transfer from ITIC to the two polymers. By comparison, it seems that the hole transfer efficiency from ITIC to PfbTAZT-BDT is a little better than that to PfbTAZT-fBDT. When excited at 600 nm, the PL of the polymers was also efficiently quenched by ITIC and has approximately the same quenching efficiency, indicating that there is efficient electron transfer from polymers to ITIC.

**Photovoltaic Properties.** To evaluate the photovoltaic properties of the polymer-based organic solar cells, ITIC has

been chosen as a small nonfullerene acceptor (A) with these two polymers (PfbTAZT-BDT or PfbTAZT-fBDT) as the donor (D) to build active layer, and the corresponding PSC devices with an inverted structure of indium tin oxide/ZnO/copolymer/ITIC/MoO<sub>3</sub>/Ag were fabricated. The active layer was spin-coated from *o*-dichlorobenzene solution with different weight ratios of D/A. First of all, three different ratios for the polymer/ITIC blends (D/A = 1.5:1, 1:1, and 1:1.5 w/w) were scanned to get the optimal D/A ratio (see Table S1 in the Supporting Information). It is found that two polymer-based devices with a blend ratio of D/A = 1:1 exhibit the best photovoltaic performances. Then, under the optimal D/A ratio, some solvent additives including 1,8-diiodooctane, diphenyl ether (DPE), and 1-chloronaphthalene were chosen to try to modify the morphologies of the active layer and to further improve the photovoltaic performances. It was found that for PfbTAZT-BDT-based device, addition of any additives fails to improve the photovoltaic performances. As for the PfbTAZT-fBDT-based device, when 2% DPE was added to the polymer/ITIC blend and the active layer was annealed for 10 min at 110 °C, the PCE is significantly increased from 5.52 to 6.59%.

The current density–voltage ( $J$ – $V$ ) curves of the two PSCs under the optimal condition are shown in Figure 4a, and the corresponding photovoltaic parameters are listed in Table 2. As can be seen, the PfbTAZT-BDT-based device shows the  $J_{sc}$  of 14.20 mA cm<sup>-2</sup>, a  $V_{oc}$  of 0.74 V, and a FF of 57.48%, leading to the PCE of 5.71%, and PfbTAZT-fBDT-based device gives a  $J_{sc}$  of 13.94 mA cm<sup>-2</sup>, a  $V_{oc}$  of 0.77 V, and a FF of 61.82%, leading to the PCE of 6.05%. By comparison, both kind of the devices shows the comparable  $J_{sc}$  for PfbTAZT-BDT ( $J_{sc}$  = 14.20 mA cm<sup>-2</sup>) and PfbTAZT-fBDT ( $J_{sc}$  = 13.94 mA cm<sup>-2</sup>) and the latter is even less than the former. However, the PfbTAZT-fBDT-based device exhibits higher  $V_{oc}$  and FF than those of the PfbTAZT-BDT. Obviously, the higher  $V_{oc}$  of the PfbTAZT-fBDT-based device is attributed to that another F atom introduced at the BDT unit reduced the HOMO energy level, which is beneficial for the enhancement of  $V_{oc}$ . In addition, the introduction of more F atoms at the conjugation skeleton is favorable to the interchain interaction and also to improve the morphologies of the active layer, thus leading to the improvement of the FF. Therefore, the best PCE of 6.59% for the PfbTAZT-fBDT-based device is higher than that of PfbTAZT-BDT (PCE = 6.04%), indicating that the introduction of F atoms onto BDT and BTAZT units has a synergistic effect on enhancing the output voltage in the device.

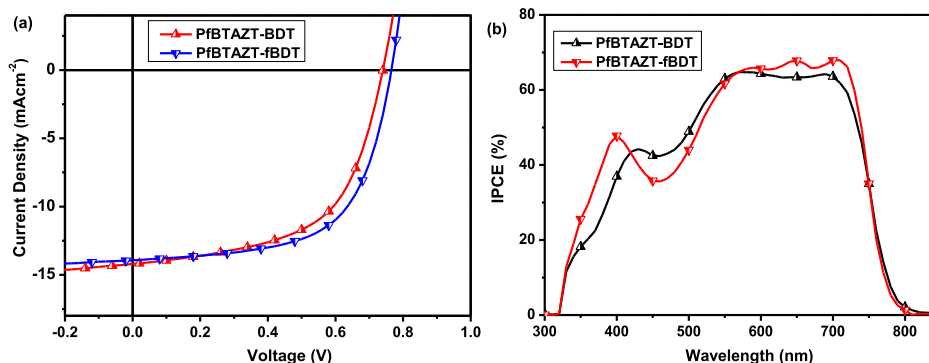
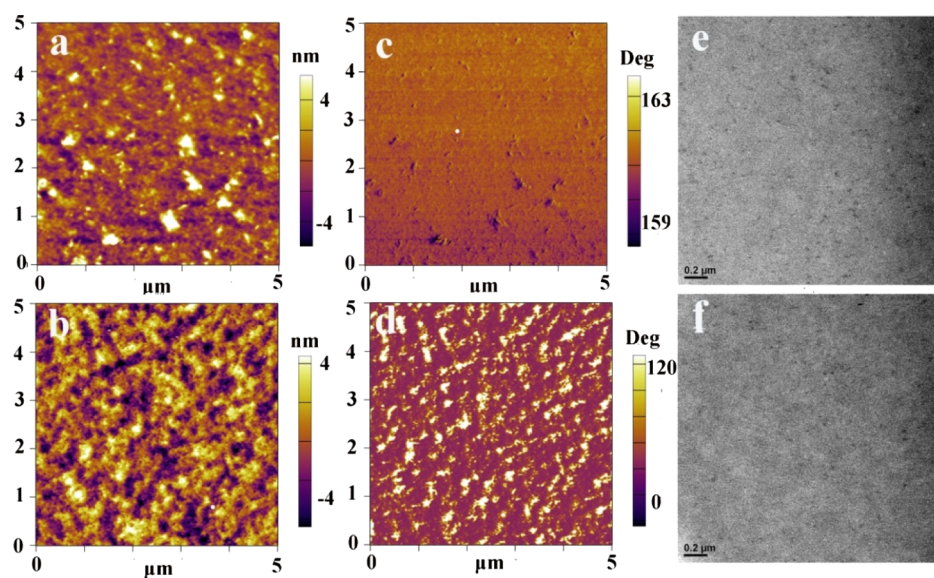


Figure 4. (a)  $J$ – $V$  curves and (b) EQE curves of the PSCs based on polymer/ITIC.

**Table 2. Photovoltaic Performance Parameters of the PSCs Based on Polymer/ITIC Blend Film under the Optimal Condition**

<sup>a</sup> device	additive	annealing	$V_{oc}$ (V)	$J_{sc}$ (mA cm <sup>-2</sup> )	FF (%)	PCE <sub>av</sub> (PCE <sub>max</sub> ) (%)
PfBTAZT-BDT/ITIC			0.74	14.20	57.48	5.71 (6.04)
PfBTAZT-fBDT/ITIC	2% DPE	110 °C	0.77	13.94	61.82	6.05 (6.59)

<sup>a</sup>Device average values and standard deviation are based on 10 devices. The best efficiencies are given in parentheses.



**Figure 5.** Tapping mode AFM height images ( $5 \times 5 \mu\text{m}^2$ ) of (a) PfBTAZT-BDT/ITIC and (b) PfBTAZT-fBDT/ITIC blend films; The AFM phase images of (c) PfBTAZT-BDT/ITIC and (d) PfBTAZT-fBDT/ITIC blend films; TEM images of (e) PfBTAZT-BDT/ITIC and (f) PfBTAZT-fBDT/ITIC blend films under the optimal condition.

Figure 4b shows incident-photon-to-converted-current efficiency (IPCE) of the PSCs fabricated under the optimal condition; the corresponding photovoltaic parameters are listed in Table 2. The IPCE of two polymer-based PSCs displays a photoresponse in the region of 350–800 nm, covering almost all of the visible region. Obviously, the IPCE for the PfBTAZT-fBDT-based device exceeds 65% from 550 to 700 nm with a peak over 67% at around 710 nm, but the maximum IPCE of 60.1% for the PfBTAZT-BDT-based device is much lower than that of PfBTAZT-fBDT, in which the PfBTAZT-BDT-based device shows a weaker photoresponse from about 350–430 and 550–750 nm but only a little stronger photoresponse in the very narrow region from about 430–550 nm, compared with the PfBTAZT-fBDT-based device. Therefore, the PfBTAZT-BDT-based device exhibits a little lower PCE than the PfBTAZT-fBDT-based device. In addition, the calculated  $J_{sc}$  values from the integration of EQE data with the AM 1.5 G reference spectrum are about 13.58 mA cm<sup>-2</sup> for PfBTAZT-BDT and 13.71 mA cm<sup>-2</sup> for PfBTAZT-fBDT, which are all within a reasonable range of error (<5%).

In order to further understand the effect of fluorinated BDT and BTAZT units on the  $J_{sc}$  and FF of the PSCs, we got the hole and electron mobility of the blend films by the space-charge-limited-current (SCLC) method (Figure S2). The hole and electron mobilities for the two blend films are shown in Table S2. The hole ( $\mu_h$ )/electron ( $\mu_e$ ) mobilities are calculated to be  $2.25 \times 10^{-4}/1.01 \times 10^{-4}$  and  $3.04 \times 10^{-4}/4.5 \times 10^{-4}$  cm<sup>2</sup> V<sup>-1</sup> s<sup>-1</sup> for PfBTAZT-BDT/ITIC blend film and PfBTAZT-fBDT/ITIC blend film, respectively. Apparently, the PfBTAZT-fBDT/ITIC blend film exhibits higher charge carrier mobilities than that of the PfBTAZT-BDT/ITIC blend

film, suggesting that the better molecular packing occurs when introducing fluorine atoms simultaneously at the BTAZT and BDT units that strengthen the intramolecular and intermolecular interactions.

**Morphological Characterization.** Atomic force microscopy (AFM) and transmission electron microscopy (TEM) were measured to evaluate the morphologies of polymer/ITIC active layer films. As can be seen in Figure 5a,b, the obtained root-mean-square (rms) roughness with 2.02 and 1.84 nm was observed for the PfBTAZT-BDT/ITIC blend film and PfBTAZT-fBDT/ITIC blend film, respectively. Because the PfBTAZT-BDT/ITIC blend film and PfBTAZT-fBDT/ITIC blend film have little different rms, they also show the comparable  $J_{sc}$ , which is in agreement with the experimental results. However, it can be seen from the AFM phase images of Figure 5c–d and TEM images of Figure 5e–f, the PfBTAZT-fBDT/ITIC blend film seems to exhibit much clearer phase separation and more uniform morphology, indicating that the PfBTAZT-fBDT/ITIC blend film has more efficient charge separation and transport ability. Thus, the PSCs based on the PfBTAZT-fBDT/ITIC blend film exhibit better FF and PCE, which is because the presence of more F atoms at the conjugation backbone does favor to strengthen the intermolecular interaction among the polymeric main chains and improve the morphologies of the polymer/ITIC blend film.

In addition, the X-ray diffraction experiment has been performed to measure the molecular packing of the two blend films (polymers/ITIC = 1:1), as shown in Figure S5. As can be seen, the PfBTAZT-fBDT/ITIC blend film obviously exhibits stronger and sharper diffraction peaks than the PfBTAZT-BDT/ITIC blend film. This implies that the intermolecular stackings for the PfBTAZT-fBDT/ITIC blend film are more

well ordered, which is favorable for improving charge transfer of the PSCs.

## CONCLUSIONS

In summary, the fBTAZT unit has been designed and synthesized and it has been applied to build two new D–A copolymers with the none/fluorine-substituted benzodithiophene (BDT) donor unit for PSCs. The measurements based on UV–vis spectroscopy and CV indicated that fluorination at both of the BTAZT unit and BDT unit shows the synergistic effect on photophysical and electrochemical properties, in which PfbBTAZT-fBDT with another F atom at the side-chain thiophene ring of the BDT unit exhibits a little more red-shift absorption and deeper HOMO–LUMO energy levels than PfbBTAZT-BDT without no F atom at the BDT unit. The photovoltaic performances of the PSCs based on the polymers as the donor and ITIC as the acceptor have been investigated, and it is found that PfbBTAZT-fBDT-based devices exhibit higher  $V_{oc}$  than the PfbBTAZT-BDT, which is attributed to its lower HOMO energy level because of more fluorine atoms introduced onto the conjugation backbone. Moreover, fluorination both into the BTAZT unit and the side-chain thiophene ring of the BDT unit in PfbBTAZT-fBDT strengthens the intermolecular interaction, which can improve the charge mobility and morphology of the active layer, thus leading to higher FF and better PCE.

## ASSOCIATED CONTENT

### Supporting Information

The Supporting Information is available free of charge on the ACS Publications website at DOI: 10.1021/acsomega.8b02053.

Instruments and measurements, device fabrication, materials and synthesis; TGA of the polymers;  $\ln(JL^3/V^2)$  versus  $(V/L)$  0.5 plots of the polymer/ITIC (1:1) film under the optimal condition of hole mobility and electron mobility by the SCLC method; the extinction coefficient of PfbBTAZT-BDT and PfbBTAZT-fBDT in  $\text{CHCl}_3$  solution; PL spectra of the polymers (excited at 600 nm) and ITIC (excited at 700 nm) films as well as the polymer/ITIC blend films of (1:1, w/w) (excited at 600 and 700 nm, respectively); X-ray diffraction patterns of the polymer/ITIC (1:1) film under the optimal condition; the solar cell parameters of the devices with different D/A ratio and with or without additive; and carrier transport properties of polymer/ITIC blend films under the optimal condition (PDF)

## AUTHOR INFORMATION

### Corresponding Authors

\*E-mail: xwzhan@pku.edu.cn (X.Z.)

\*E-mail: xgchen@whu.edu.cn (X.C.)

### ORCID

Xiaowei Zhan: 0000-0002-1006-3342

Xingguo Chen: 0000-0002-0221-733X

### Notes

The authors declare no competing financial interest.

## ACKNOWLEDGMENTS

This work was supported by the Science and Technology Department of Hubei Province (no. 2018AAA013).

## REFERENCES

- (1) Yu, G.; Gao, J.; Hummelen, J. C.; Wudl, F.; Heeger, A. J. Polymer photovoltaic cells: enhanced efficiencies via a network of internal donor-acceptor heterojunctions. *Science* **1995**, *270*, 1789–1791.
- (2) Li, G.; Zhu, R.; Yang, Y. Polymer solar cells. *Nat. Photonics* **2012**, *6*, 153–161.
- (3) Machui, F.; Hösel, M.; Li, N.; Spyropoulos, G. D.; Ameri, T.; Sondergaard, R. R.; Jørgensen, M.; Scheel, A.; Gaiser, D.; Kreul, K.; Lenssen, D.; Legros, M.; Lemaitre, N.; Vilkmann, M.; Välimäki, M.; Nordman, S.; Brabec, C. J.; Krebs, F. C. Cost analysis of roll-to-roll fabricated ITO free single and tandem organic solar modules based on data from manufacture. *Energy Environ. Sci.* **2014**, *7*, 2792–2802.
- (4) Li, Y. Molecular design of photovoltaic materials for polymer solar cells: toward suitable electronic energy levels and broad absorption. *Acc. Chem. Res.* **2012**, *45*, 723–733.
- (5) Günes, S.; Neugebauer, H.; Sariciftci, N. S. Conjugated polymer-based organic solar cells. *Chem. Rev.* **2007**, *107*, 1324–1338.
- (6) Liu, Y.; Zhao, J.; Li, Z.; Mu, C.; Ma, W.; Hu, H.; Jiang, K.; Lin, H.; Ade, H.; Yan, H. Aggregation and morphology control enables multiple cases of high-efficiency polymer solar cells. *Nat. Commun.* **2014**, *5*, 5293–5301.
- (7) Holliday, S.; Ashraf, R. S.; Wadsworth, A.; Baran, D.; Yousaf, S. A.; Nielsen, C. B.; Tan, C.-H.; Dimitrov, S. D.; Shang, Z.; Gasparini, N.; Alamoudi, M.; Laquai, F.; Brabec, C. J.; Salbeck, A.; Durrant, J. R.; McCulloch, I. High-efficiency and air-stable P3HT-based polymer solar cells with a new non-fullerene acceptor. *Nat. Commun.* **2016**, *7*, 11585–11595.
- (8) Dai, S.; Zhao, F.; Zhang, Q.; Lau, T.-K.; Li, T.; Liu, K.; Ling, Q.; Wang, C.; Lu, X.; You, W.; Zhan, X. Fused nonacyclic electron acceptors for efficient polymer solar cells. *J. Am. Chem. Soc.* **2017**, *139*, 1336–1343.
- (9) Liu, F.; Zhou, Z.; Zhang, C.; Vergote, T.; Fan, H.; Liu, F.; Zhu, X. A Thieno[3,4-b]thiophene-Based Non-fullerene Electron Acceptor for High-Performance Bulk-Heterojunction Organic Solar Cells. *J. Am. Chem. Soc.* **2016**, *138*, 15523–15526.
- (10) Zhao, W.; Li, S.; Yao, H.; Zhang, S.; Zhang, Y.; Yang, B.; Hou, J. Molecular optimization enables over 13% efficiency in organic solar cells. *J. Am. Chem. Soc.* **2017**, *139*, 7148–7151.
- (11) Li, S.; Ye, L.; Zhao, W.; Yan, H.; Yang, B.; Liu, D.; Li, W.; Ade, H.; Hou, J. A Wide Band-Gap Polymer with a Deep HOMO Level Enables 14.2% Efficiency in Polymer Solar Cells. *J. Am. Chem. Soc.* **2018**, *140*, 7159.
- (12) Fei, Z.; Eisner, F. D.; Jiao, X.; Azzouzi, M.; Röhr, J. A.; Han, Y.; Shahid, M.; Chesman, A. S. R.; Easton, C. D.; McNeill, C. R.; Anthopoulos, T. D.; Nelson, J.; Heeney, M. An Alkylated Indacenodithieno [3, 2-b] thiophene-Based Nonfullerene Acceptor with High Crystallinity Exhibiting Single Junction Solar Cell Efficiencies Greater than 13% with Low Voltage Losses. *Adv. Mater.* **2018**, *30*, 1705209.
- (13) Sun, J.; Ma, X.; Zhang, Z.; Yu, J.; Zhou, J.; Yin, X.; Yang, L.; Geng, R.; Zhu, R.; Zhang, F.; Tang, W. Dithieno [3, 2-b: 2', 3'-d'] pyrrol Fused Nonfullerene Acceptors Enabling Over 13% Efficiency for Organic Solar Cells. *Adv. Mater.* **2018**, *30*, 1707150.
- (14) Zhu, J.; Xiao, Y.; Wang, J.; Liu, K.; Jiang, H.; Lin, Y.; Lu, X.; Zhan, X. Alkoxy-Induced Near-Infrared Sensitive Electron Acceptor for High-Performance Organic Solar Cells. *Chem. Mater.* **2018**, *30*, 4150–4156.
- (15) Wang, J.; Zhang, J.; Xiao, Y.; Xiao, T.; Zhu, R.; Yan, C.; Fu, Y.; Lu, G.; Lu, X.; Marder, S. R.; Zhan, X. Effect of Isomerization on High-Performance Nonfullerene Electron Acceptors. *J. Am. Chem. Soc.* **2018**, *140*, 9140–9147.
- (16) Chen, J.-D.; Li, Y.-Q.; Zhu, J.; Zhang, Q.; Xu, R.-P.; Li, C.; Zhang, Y.-X.; Huang, J.-S.; Zhan, X.; You, W.; Tang, J.-X. Polymer Solar Cells with 90% External Quantum Efficiency Featuring an Ideal Light-and Charge-Manipulation Layer. *Adv. Mater.* **2018**, *30*, 1706083.

- (17) Nielsen, C. B.; Holliday, S.; Chen, H.-Y.; Cryer, S. J.; McCulloch, I. Non-fullerene electron acceptors for use in organic solar cells. *Acc. Chem. Res.* **2015**, *48*, 2803–2812.
- (18) Zhao, F.; Dai, S.; Wu, Y.; Zhang, Q.; Wang, J.; Jiang, L.; Ling, Q.; Wei, Z.; Ma, W.; You, W.; Wang, C.; Zhan, X. Single-Junction Binary-Blend Nonfullerene Polymer Solar Cells with 12.1% Efficiency. *Adv. Mater.* **2017**, *29*, 1700144.
- (19) Lin, Y.; Zhan, X. Oligomer molecules for efficient organic photovoltaics. *Acc. Chem. Res.* **2015**, *49*, 175–183.
- (20) Lin, Y.; Zhan, X. Non-fullerene acceptors for organic photovoltaics: an emerging horizon. *Mater. Horiz.* **2014**, *1*, 470–488.
- (21) Liu, Y.; Zhang, Z.; Feng, S.; Li, M.; Wu, L.; Hou, R.; Xu, X.; Chen, X.; Bo, Z. Exploiting noncovalently conformational locking as a design strategy for high performance fused-ring electron acceptor used in polymer solar cells. *J. Am. Chem. Soc.* **2017**, *139*, 3356–3359.
- (22) Dai, S.; Li, T.; Wang, W.; Xiao, Y.; Lau, T.-K.; Li, Z.; Liu, K.; Lu, X.; Zhan, X. Enhancing the Performance of Polymer Solar Cells via Core Engineering of NIR-Absorbing Electron Acceptors. *Adv. Mater.* **2018**, *30*, 1706571.
- (23) Li, T.; Dai, S.; Ke, Z.; Yang, L.; Wang, J.; Yan, C.; Ma, W.; Zhan, X. Fused Tris(thienothiophene)-Based Electron Acceptor with Strong Near-Infrared Absorption for High-Performance As-Cast Solar Cells. *Adv. Mater.* **2018**, *30*, 1705969.
- (24) Yan, C.; Barlow, S.; Wang, Z.; Yan, H.; Jen, A. K.-Y.; Marder, S. R.; Zhan, X. Non-fullerene acceptors for organic solar cells. *Nat. Rev. Mater.* **2018**, *3*, 18003.
- (25) Li, S.; Zhan, L.; Liu, F.; Ren, J.; Shi, M.; Li, C.-Z.; Russell, T. P.; Chen, H. An Unfused-Core-Based Nonfullerene Acceptor Enables High-Efficiency Organic Solar Cells with Excellent Morphological Stability at High Temperatures. *Adv. Mater.* **2018**, *30*, 1705208.
- (26) Yao, Z.; Liao, X.; Gao, K.; Lin, F.; Xu, X.; Shi, X.; Zuo, L.; Liu, F.; Chen, Y.; Jen, A. K.-Y. Dithienopicenocarbazole-Based Acceptors for Efficient Organic Solar Cells with Optoelectronic Response Over 1000 nm and an Extremely Low Energy Loss. *J. Am. Chem. Soc.* **2018**, *140*, 2054–2057.
- (27) Li, X.; Huang, H.; Bin, H.; Peng, Z.; Zhu, C.; Xue, L.; Zhang, Z.-G.; Zhang, Z.; Ade, H.; Li, Y. Synthesis and Photovoltaic Properties of a Series of Narrow Bandgap Organic Semiconductor Acceptors with Their Absorption Edge Reaching 900 nm. *Chem. Mater.* **2017**, *29*, 10130–10138.
- (28) Wu, Y.; Bai, H.; Wang, Z.; Cheng, P.; Zhu, S.; Wang, Y.; Ma, W.; Zhan, X. A planar electron acceptor for efficient polymer solar cells. *Energy Environ. Sci.* **2015**, *8*, 3215–3221.
- (29) Lin, Y.; Zhao, F.; He, Q.; Huo, L.; Wu, Y.; Parker, T. C.; Ma, W.; Sun, Y.; Wang, C.; Zhu, D.; Heeger, A. J.; Marder, S. R.; Zhan, X. High-performance electron acceptor with thienyl side chains for organic photovoltaics. *J. Am. Chem. Soc.* **2016**, *138*, 4955–4961.
- (30) Cheng, P.; Li, G.; Zhan, X.; Yang, Y. Next-generation organic photovoltaics based on non-fullerene acceptors. *Nat. Photonics* **2018**, *12*, 131–142.
- (31) Zhu, J.; Ke, Z.; Zhang, Q.; Wang, J.; Dai, S.; Wu, Y.; Xu, Y.; Lin, Y.; Ma, W.; You, W.; Zhan, X. Naphthodithiophene-Based Non-fullerene Acceptor for High-Performance Organic Photovoltaics: Effect of Extended Conjugation. *Adv. Mater.* **2018**, *30*, 1704713.
- (32) Wang, J.; Wang, W.; Wang, X.; Wu, Y.; Zhang, Q.; Yan, C.; Ma, W.; You, W.; Zhan, X. Enhancing Performance of Nonfullerene Acceptors via Side-Chain Conjugation Strategy. *Adv. Mater.* **2017**, *29*, 1702125.
- (33) Wang, W.; Yan, C.; Lau, T.-K.; Wang, J.; Liu, K.; Fan, Y.; Lu, X.; Zhan, X. Fused Hexacyclic Nonfullerene Acceptor with Strong Near-Infrared Absorption for Semitransparent Organic Solar Cells with 9.77% Efficiency. *Adv. Mater.* **2017**, *29*, 1701308.
- (34) Lin, Y.; Wang, J.; Zhang, Z.-G.; Bai, H.; Li, Y.; Zhu, D.; Zhan, X. An electron acceptor challenging fullerenes for efficient polymer solar cells. *Adv. Mater.* **2015**, *27*, 1170–1174.
- (35) Lin, Y.; Zhang, Z.-G.; Bai, H.; Wang, J.; Yao, Y.; Li, Y.; Zhu, D.; Zhan, X. High-performance fullerene-free polymer solar cells with 6.31% efficiency. *Energy Environ. Sci.* **2015**, *8*, 610–616.
- (36) Lin, Y.; He, Q.; Zhao, F.; Huo, L.; Mai, J.; Lu, X.; Su, C.-J.; Li, T.; Wang, J.; Zhu, J.; Sun, Y.; Wang, C.; Zhan, X. A facile planar fused-ring electron acceptor for as-cast polymer solar cells with 8.71% efficiency. *J. Am. Chem. Soc.* **2016**, *138*, 2973–2976.
- (37) Lin, Y.; Zhao, F.; Prasad, S. K. K.; Chen, J.-D.; Cai, W.; Zhang, Q.; Chen, K.; Wu, Y.; Ma, W.; Gao, F.; Tang, J.-X.; Wang, C.; You, W.; Hodgkiss, J. M.; Zhan, X. Balanced Partnership between Donor and Acceptor Components in Nonfullerene Organic Solar Cells with >12% Efficiency. *Adv. Mater.* **2018**, *30*, 1706363.
- (38) Lin, Y.; Zhao, F.; Wu, Y.; Chen, K.; Xia, Y.; Li, G.; Prasad, S. K. K.; Zhu, J.; Huo, L.; Bin, H.; Zhang, Z.-G.; Guo, X.; Zhang, M.; Sun, Y.; Gao, F.; Wei, Z.; Ma, W.; Wang, C.; Hodgkiss, J.; Bo, Z.; Inganäs, O.; Li, Y.; Zhan, X. Mapping Polymer Donors toward High-Efficiency Fullerene Free Organic Solar Cells. *Adv. Mater.* **2017**, *29*, 1604155.
- (39) Fan, B.; Zhang, K.; Jiang, X.-F.; Ying, L.; Huang, F.; Cao, Y. High-Performance Nonfullerene Polymer Solar Cells based on Imide-Functionalized Wide-Bandgap Polymers. *Adv. Mater.* **2017**, *29*, 1606396.
- (40) Huo, L.; Liu, T.; Sun, X.; Cai, Y.; Heeger, A. J.; Sun, Y. Single-Junction Organic Solar Cells Based on a Novel Wide-Bandgap Polymer with Efficiency of 9.7%. *Adv. Mater.* **2015**, *27*, 2938–2944.
- (41) Li, Y.; Zhong, L.; Gautam, B.; Bin, H.-J.; Lin, J.-D.; Wu, F.-P.; Zhang, Z.; Jiang, Z.-Q.; Zhang, Z.-G.; Gundogdu, K.; Li, Y.; Liao, L.-S. A near-infrared non-fullerene electron acceptor for high performance polymer solar cells. *Energy Environ. Sci.* **2017**, *10*, 1610–1620.
- (42) Yang, Y.; Zhang, Z.-G.; Bin, H.; Chen, S.; Gao, L.; Xue, L.; Yang, C.; Li, Y. Side-chain isomerization on an n-type organic semiconductor ITIC acceptor makes 11.77% high efficiency polymer solar cells. *J. Am. Chem. Soc.* **2016**, *138*, 15011–15018.
- (43) Fan, Q.; Su, W.; Meng, X.; Guo, X.; Li, G.; Ma, W.; Zhang, M.; Li, Y. High-Performance Non-Fullerene Polymer Solar Cells Based on Fluorine Substituted Wide Bandgap Copolymers Without Extra Treatments. *Sol. RRL* **2017**, *1*, 1700020.
- (44) Yao, H.; Cui, Y.; Yu, R.; Gao, B.; Zhang, H.; Hou, J. Design, Synthesis, and Photovoltaic Characterization of a Small Molecular Acceptor with an Ultra-Narrow Band Gap. *Angew. Chem., Int. Ed.* **2017**, *56*, 3045–3049.
- (45) Zhang, Z.-G.; Wang, J. Structures and properties of conjugated Donor-Acceptor copolymers for solar cell applications. *J. Mater. Chem.* **2012**, *22*, 4178–4187.
- (46) Zhang, Z.-G.; Li, Y. Side-chain engineering of high-efficiency conjugated polymer photovoltaic materials. *Sci. China: Chem.* **2015**, *58*, 192–209.
- (47) Reichenbacher, K.; Süß, H. I.; Hulliger, J. Fluorine in crystal engineering—"the little atom that could". *Chem. Soc. Rev.* **2005**, *34*, 22–30.
- (48) Wang, Z.; Xu, X.; Li, Z.; Feng, K.; Li, K.; Li, Y.; Peng, Q. Solution-Processed Organic Solar Cells with 9.8% Efficiency Based on a New Small Molecule Containing a 2D Fluorinated Benzodithiophene Central Unit. *Adv. Electron. Mater.* **2016**, *2*, 1600061.
- (49) Schroeder, B. C.; Huang, Z.; Ashraf, R. S.; Smith, J.; D'Angelo, P.; Watkins, S. E.; Anthopoulos, T. D.; Durrant, J. R.; McCulloch, I. Silindacenodithiophene-Based Low Band Gap Polymers - The Effect of Fluorine Substitution on Device Performances and Film Morphologies. *Adv. Funct. Mater.* **2012**, *22*, 1663–1670.
- (50) Liu, P.; Zhang, K.; Liu, F.; Jin, Y.; Liu, S.; Russell, T. P.; Yip, H.-L.; Huang, F.; Cao, Y. Effect of Fluorine Content in Thienothiophene-Benzodithiophene Copolymers on the Morphology and Performance of Polymer Solar Cells. *Chem. Mater.* **2014**, *26*, 3009–3017.
- (51) Xue, L.; Yang, Y.; Xu, J.; Zhang, C.; Bin, H.; Zhang, Z.-G.; Qiu, B.; Li, X.; Sun, C.; Gao, L.; Yao, J.; Chen, X.; Yang, Y.; Xiao, M.; Li, Y. Side Chain Engineering on Medium Bandgap Copolymers to Suppress Triplet Formation for High-Efficiency Polymer Solar Cells. *Adv. Mater.* **2017**, *29*, 1703344.
- (52) Liu, D.; Zhao, W.; Zhang, S.; Ye, L.; Zheng, Z.; Cui, Y.; Chen, Y.; Hou, J. Highly efficient photovoltaic polymers based on benzodithiophene and quinoxaline with deeper HOMO levels. *Macromolecules* **2015**, *48*, 5172–5178.

(53) Lee, J.; Kim, M.; Kang, B.; Jo, S. B.; Kim, H. G.; Shin, J.; Cho, K. Side-Chain Engineering for Fine-Tuning of Energy Levels and Nanoscale Morphology in Polymer Solar Cells. *Adv. Energy Mater.* **2014**, *4*, 1400087.

(54) Wang, Y.; Fan, Q.; Guo, X.; Li, W.; Guo, B.; Su, W.; Ou, X.; Zhang, M. High-performance nonfullerene polymer solar cells based on a fluorinated wide bandgap copolymer with a high open-circuit voltage of 1.04 V. *J. Mater. Chem. A* **2017**, *5*, 22180–22185.

(55) Zhang, G.; Xu, X.; Bi, Z.; Ma, W.; Tang, D.; Li, Y.; Peng, Q. Fluorinated and Alkylthiolated Polymeric Donors Enable both Efficient Fullerene and Nonfullerene Polymer Solar Cells. *Adv. Funct. Mater.* **2018**, *28*, 1706404.

(56) Zhang, M.; Guo, X.; Zhang, S.; Hou, J. Synergistic effect of fluorination on molecular energy level modulation in highly efficient photovoltaic polymers. *Adv. Mater.* **2014**, *26*, 1118–1123.

(57) Zhou, P.; Zhang, Z.-G.; Li, Y.; Chen, X.; Qin, J. Thiophene-Fused Benzothiadiazole: A Strong Electron-Acceptor Unit to Build D-A Copolymer for Highly Efficient Polymer Solar Cells. *Chem. Mater.* **2014**, *26*, 3495–3501.

(58) Zhou, P.; Yang, Y.; Chen, X.; Zhang, Z.-G.; Li, Y. Design of a thiophene-fused benzotriazole unit as an electron acceptor to build D-A copolymers for polymer solar cells. *J. Mater. Chem. C* **2017**, *5*, 2951–2957.

(59) Jiang, X.; Yang, Y.; Zhu, J.; Lau, T.-K.; Cheng, P.; Lu, X.; Zhan, X.; Chen, X. Constructing D-A copolymers based on thiophene-fused benzotriazole units containing different alkyl side-chains for non-fullerene polymer solar cells. *J. Mater. Chem. C* **2017**, *5*, 8179–8186.

(60) Zhang, M.; Guo, X.; Ma, W.; Ade, H.; Hou, J. A Large-Bandgap Conjugated Polymer for Versatile Photovoltaic Applications with High Performance. *Adv. Mater.* **2015**, *27*, 4655–4660.

(61) Meng, H.; Wudl, F. A Robust Low Band Gap Processable n-Type Conducting Polymer Based on Poly(isothianaphthene). *Macromolecules* **2001**, *34*, 1810–1816.

(62) Liang, Y.; Feng, D.; Guo, J.; Szarko, J. M.; Ray, C.; Chen, L. X.; Yu, L. Regioregular Oligomer and Polymer Containing Thieno[3,4-*b*]thiophene Moiety for Efficient Organic Solar Cells. *Macromolecules* **2009**, *42*, 1091–1098.